RESEARCH ARTICLE

Relationships between carbon fluxes and environmental factors in a drip-irrigated, film-mulched cotton field in arid region

Xiaoyu Li[1,2], Lijuan Liu[1], Huijin Yang[3], Yan Li[1]*

1 State Key Laboratory of Subtropical Silviculture, Zhejiang A&F University, Lin'an, China, **2** Xinjiang Institute of Ecology and Geography, Chinese Academy of Sciences, Xinjiang, China, **3** School of Remote Sensing and Information Engineering, Wuhan University, Wuhan, China

* liyan2016@zafu.edu.cn

Abstract

Environmental factors and human activities play important roles in carbon fixation and emissions generated from croplands. Eddy covariance measurements in a drip-irrigated, film-mulched cotton field were used to analyze the relationships between carbon fluxes and environmental factors in Wulanwusu, northern Xinjiang, an arid region of Northwest China. Our results showed that the cumulative net carbon flux (NEE) was -304.8 g C m^{-2} (a strong sink) over the whole cotton growing season in 2012, which was more than that in cotton cropland without plastic film mulching and drip-irrigation. Moreover, when time is scaled up from a half-hour to a month, the correlations of gross primary production (GPP) to air temperature (T_{air}), net solar radiation (R_n) and soil water content (SWC) gradually become stronger due to ecosystem resistance and resilience as well as the protection of plastic film mulching. The GPP is more strongly correlated with R_n than T_{air} at time scales from minutes to days, while it reverses at time scales from days to weeks. This outcome is largely determined by the biochemical characteristics of photosynthesis. SWC and vapor pressure deficit (VPD) at all time scales are weakly correlated with GPP because plastic film mulching and regularly drip-irrigation allow soil to maintain sufficient water.

Introduction

Carbon dioxide emissions generated from upland agro-ecosystems are a major source of atmospheric greenhouse gases [1]. Agricultural lands occupy 37% of the Earth's land surface and account for 20% of atmospheric carbon dioxide [2]. Additionally, agricultural lands are a non-ignorable carbon sink. Conversely, an elevated concentration of atmosphere carbon dioxide could have a large impact on future agricultural productivity [3–5], as it can accelerate agricultural crop growth rates [6,7]. Consequently, measurements of carbon fluxes generated from agro-ecosystems in an arid region are essential to an analysis of carbon flux dynamics.

Agricultural lands are extremely important in oases of Xinjiang, an extensive arid region of Northwest China. Although oases account for only 4–5% of the total area of this region, over 90% of the province's population and 95% of its wealth are concentrated within them [8]. The

Manas River Watershed is a typical mountain-oasis-desert ecosystem in the arid region of Northwest China. The rapid growth of the regional population and the continuous expansion of agricultural lands in this watershed induce acute and frequent water shortages [8,9]. The agricultural water consumption currently accounts for 96.2% of the total water consumption in this watershed [8]. Therefore, water-saving irrigation is of great importance in this arid region. The intensifying human exploitation in this watershed is typical in the arid region of Northwest China [9,10].

Mulched-drip irrigation is a great approach to save water. Drip irrigation was combined with film mulching successfully in 1996 after the Eighth Agricultural Division of Xinjiang Production and Construction Corps, which is located in the Manas River Watershed, experimented with the combined technology in a small area. It has been widely promoted and applied since 1999, and now, the cropland covered by plastic film mulching with drip irrigation accounts for up to 80% of the total irrigated area in the Manas River Watershed. It has widely taken the place of the traditional furrow irrigation and is the predominant irrigation method in recent years in the most of China's arid regions [11]. Additionally, the Manas River Watershed is the biggest cotton belt in Xinjiang, with a cotton-planting area of up to 52% of the agricultural land. Therefore, cotton fields in this watershed can be considered representative of the entire arid region, with the utilization of plastic film mulching and drip irrigation key issues.

Plastic film mulching with drip irrigation alters the soil microenvironment and has a great impact on the agro-ecosystem, bringing with it many advantages such as weed inhibition, soil temperature improvement, water evaporation reduction, soil organic carbon stock enhancement, greenhouse gas emission reductions and crop yield increase [12–16]. The impact of partial surface mulch on soil heat and water flow was examined by many studies [17–19]. More recently, some researchers have compared the effects of flood irrigation without film mulching and plastic film mulching with drip irrigation on carbon and water fluxes in arid or semi-arid regions [12, 14, 16, 20, 21]. Some studies have also shown that plastic film mulching with drip irrigation has great effects on nitrous oxide and methane emissions in arid regions [11, 13, 22, 23]. For example, Berger et al. (2013) [23] contended that polyethylene mulching may decrease nitrous oxide emissions. Additionally, there exist some studies concerning the relationships of carbon fluxes with environmental factors (R_n, T_{air}, VPD and SWC) [24–31]. Vourlitis et al (2000) [32] and Whitley et al. (2009) [33] discussed the responses of stand transpiration to R_n, VPD and SWC at different time scales, and Liu et al. (2009) [21] analyzed the correlations between temperature and carbon fluxes in different types of film mulching. However, these studies have only concentrated on the influences of plastic film mulching with drip irrigation on soil water, greenhouse gas emission and crop yield, and so on; there is still a lack of information about the quantitative analyses of the relationships between carbon fluxes and environmental factors under the influence of plastic film mulching with drip irrigation at various time scales. Consequently, in a drip-irrigated, film-mulched cotton field, analysis of their relationships is essential to understanding the influence of environmental factors on carbon fluxes [5], and provides the scientific basis for emphasizing different environmental factors at different time scales.

Materials and methods

Site description

The study site (latitude 44˚17′N, longitude 85˚49′E, elevation 468.2 m) is located at the Wulanwusu Agrometeorological Experiment Station on the northern slope of the Tianshan Mountains in Xinjiang, Northwest China. This region is subject to a typical temperate continental

climate. Using 30 years (1980–2010) of climatology data from a meteorological dataset, the precipitation shows large fluctuations, varying from 71.95 to 242.3 mm, with an average precipitation of 129.88 mm over the growing season. The mean length of the full growing season is approximately 169 days. The mean annual sunshine duration is 2861 hours per year with approximately 170 frost-free days [8]. The soil type is gray desert soil, consisting of 42% silt, 39% sand and 19% clay at 0–30 mm depth. The mean field moisture capacity is 27.1%, and the bulk density is approximately 1.3 g cm^{-3} [8]. Furthermore, the average T_{air} and precipitation was 22.42˚C and 50.5 mm in the 2012 growing season.

The experimental plot at the station is 39600 m^2 (300m×120m) and is flat enough for cotton with a mean population density of approximately 24 plants m^{-2}. The cotton in the experimental plot was sowed on April 17 and harvested on September 23, 2012 (the entire growth period of cotton is 158 days). The field management of cotton was in accordance with local practices to ensure a realistic characterization of NEE and GPP from an agricultural area in this watershed; 80% of this plot is covered with plastic film mulching of 0.08 mm thickness; a drip hose was placed under the plastic film, an irrigation method referred to as 'film-mulched drip irrigation' [8]. Plastic film mulching is kept on the field from cotton sowing to harvesting.

Eddy covariance flux measurement

An eddy covariance (EC) system is located in a cotton field with relatively homogeneous and adequate fetch. Data (including carbon fluxes, sensible heat fluxes and latent heat fluxes) were established in 2009. Data from 17 April 2012 to 23 September 2012 are used in this study. The site was equipped with a three-dimensional sonic anemometer (CSAT3, Campbell, USA) for measuring wind speed and wind direction and an open-path infrared CO2/H2O analyzer (IRGA, LI-7500, Li-Cor, USA) for measuring carbon dioxide and water vapor concentrations on a mast at a 4-m height. Furthermore, the flux mast was also equipped with some additional sensors. R_n is measured with a CNR1 (Kipp & Zonen,Netherlands), T_{air} and air humidity with a HMP45C (Vaisala, Helsinki, Finland), soil heat flux with two HFP01 sensors (Hukseflux, Netherlands) and soil temperature with four Thermocouples (TCAV, Campbell, USA). Data measured by these sensors can be recorded automatically at 10 Hz on a data logger (CR3000, Campbell, USA).

Data processing

The eddy covariance method was applied during steady atmospheric conditions and on relatively flat terrain; otherwise, it would be vulnerable to systematic bias errors [34]. Therefore, we filtered some outliers and fill gaps to improve the quality of the trace gas fluxes.

Using the EddyPro software, these data were corrected by performing the following: three-axis coordinate rotations to eliminate errors due to sensor tilt relative to the terrain surface [35, 36]; WPL correction to compensate for the fluctuations of temperature and water vapor due to the presence of heat and water vapor flux [37,38]; and spectral corrections to compensate for the spectral attenuation due to the separation between sensors [39].

To minimize data errors, we screened the data, the process of which consisted of two steps. First, the outliers were detected by the comparison of half-hourly fluxes X_i with a 200-data point moving mean (X_{gi}) and standard deviation (X_{sdi}) [40]:if

$$X_i < X_{gi} - (2.5 \times X_{sdi}) \tag{1}$$

or

$$X_i > X_{gi} + (2.5 \times X_{sdi}) \tag{2}$$

then X_i was screened from the dataset. In addition, the data of daytime and nighttime were screened separately. Nighttime was defined as a downward solar radiation < 20 Wm^{-2}[41].

Second, nighttime NEE that were less than 0 and larger than 0.6 mg C m^{-2}s^{-1}werealso screened [42,43]. However, the condition of low turbulence at night [44] could have caused the nighttime fluxes to be underestimated [45–48]. Accordingly, if Ustar is less than 0.15 ms^{-1}, as determined by an average values test (AVT) [43], then the NEE that corresponds to these Ustar are screened.

After screening, approximately 82% of the trace gas fluxes remained. However, these incomplete data were not enough for further analysis. Thus, to accurately calculate values of trace gas fluxes, gap-filling was imperative. In this study, we filled gaps using the online eddy covariance processing tool of the Department of Biogeochemical Integration at the Max Planck Institute for Biogeochemistry (http://www.bgc-jena.mpg.de/~MDIwork/eddyproc/).

Flux-partitioning

NEE exchange is partitioned into two components, GPP and R_{eco} [28,47]:

$$NEE = R_{eco} - GPP \tag{3}$$

The R_{eco} and NEE were calculated by the online eddy covariance processing tool of the Department of Biogeochemical Integration at the Max Planck Institute for Biogeochemistry (http://www.bgc-jena.mpg.de/~MDIwork/eddyproc/).

Response functions of GPP

R_n, T_{air}, and SWC are the primary environmental factors that affect ecosystem carbon uptake and release[30,32,49].

We assessed the relationship between GPP and T_{air} using the nonlinear fitting function [50,51]:

$$y = a \times \exp(-k_1 \times (x - k_3)^2/(x + k_2)) \tag{4}$$

where y represents GPP; x is VPD or T_{air}; a is the maximum value of GPP (GPP$_{max}$); k_1 and k_2 represent the shape of the response curve; and k_3 describes the value of the VPD or T_{air} at which GPP is maximized.

To study the responses of the GPP to R_n at the half-hourly time scale, we used the asymptote equation to obtain light–response curves [33,51]:

$$y = a \times x/(x + b) \tag{5}$$

where y represents GPP; x is R_n; a is the light saturation GPP (GPP$_{max}$); and b is the rate of change.

At half-monthly and monthly time scales, the responses of GPP to T_{air} and R_n are described using linear relationships with log-transformed data, $\ln(y) = ax + b$, which is similar to the response of R_{eco} against T_{soil} [25].

Data quality assessment

According to the first law of thermodynamics, the sum of the estimated latent and sensible heat flux must be equivalent to all other energy sinks and sources, and energy balance closure can be expressed as[42,52]

$$LE + H = R_n - G - S - Q \tag{6}$$
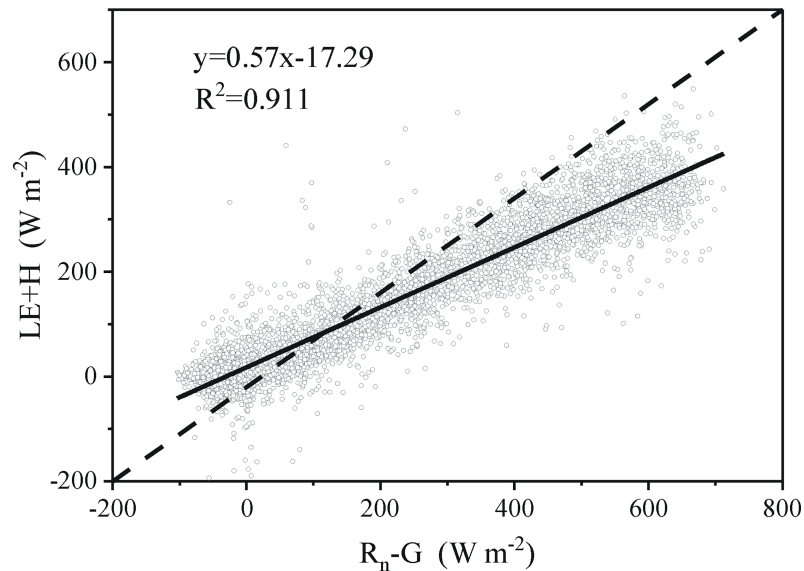
Fig 1. Energy-balance closure of cotton during entire growth period. The slope of the solid line represents the degree of energy balance closure. (R_n is the net radiation, G the soil heat flux, LE is the latent heat flux, H is the sensible heat flux).

where R_n is the net radiation, LE the latent heat flux, H the sensible heat flux, S canopy heat storage, G the soil heat flux, and Q the sum of all additional energy sources. Q is neglected as a small term. Canopy heat storage can also be neglected in short canopies on the condition of the vegetation height being less than 8 m[52].

The slope of LE+H against R_n-G is 0.57 (Fig 1) over the entire growing season; the energy balance is not closed.

The data shown in all figures, and supporting all of the principal results in this paper, are publicly available:

(http://www.editorialmanager.com/pone/download.aspx?id = 21540143&guid = 5ccdf696-9d97-471f-b758-4704b73813ed&scheme = 1).

Results

Diurnal variations in NEE

The mean diurnal variations in NEE during each of the growth stages of cotton are shown in Fig 2. We calculated the random uncertainty of each data point. For example, during the sowing period, the random uncertainty of NEE at 12:00 am represented the standard deviation of all of NEE at this time and growth stage; the uncertainty is equal to the error bars given in Fig 2.

Overall, the dynamic of NEE in all growing stages shows a single-peak curve. In the periods of seeding emergence and boll opening, NEE is positive at night due only to respiration and is negative in the day predominantly due to photosynthesis. The absolute value of NEE is largest at midday due to sufficient solar radiation and high temperatures.

NEE has a conspicuous distinction at different growth stages; the absolute value of NEE during the sowing period (Fig 2A) is the lowest of all five growth stages due to the absence of photosynthesis and depending on the respiration. The day length of carbon fixation is longest in the periods of squaring, flowering and boll formation (14 hours, Fig 2D). Carbon fixation in
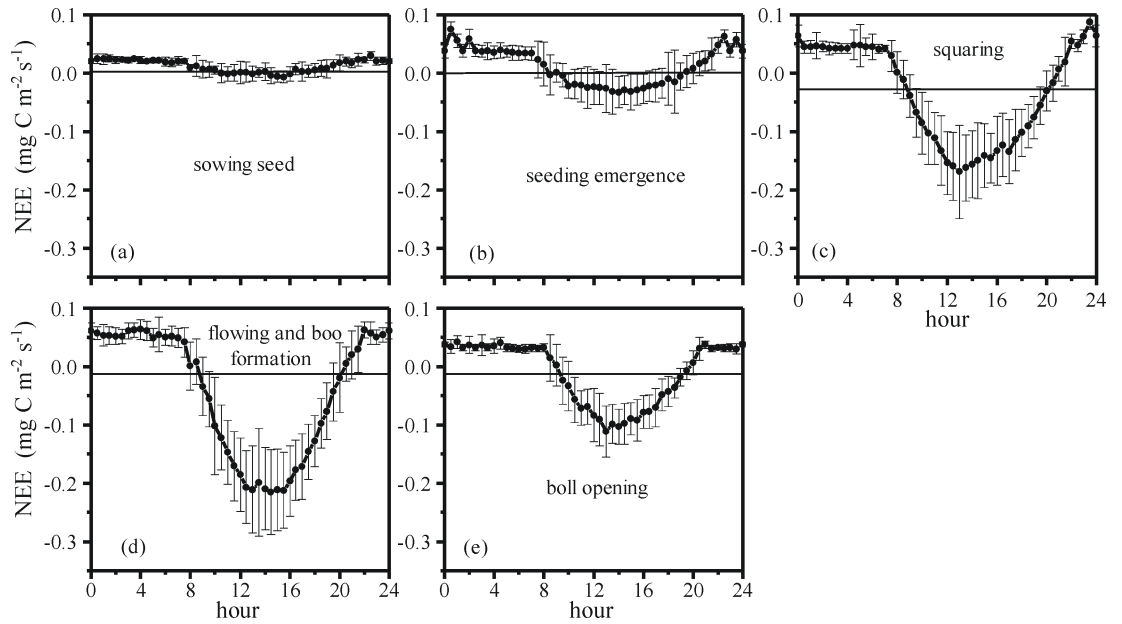
Fig 2. Average diurnal profiles of NEE (net ecosystem exchange) for five growth stages and mean values of the diurnal variation in NEE for each growth stages. The vertical bars represent the standard deviation of the mean values.

the squaring (Fig 2C) begins early in the morning (approximately at 8 am), but carbon fixation in seeding emergence is delayed by approximately 0.5 hours (Fig 2B).

Carbon sink or source

The cotton field is a strong sink of carbon over the growing season as a whole, as illustrated in Fig 3. Over the entire growing season, cumulative NEE first increases and then decreases (Fig 3). From the beginning of sowing to the end of the seed emergence, NEE is positive, and the
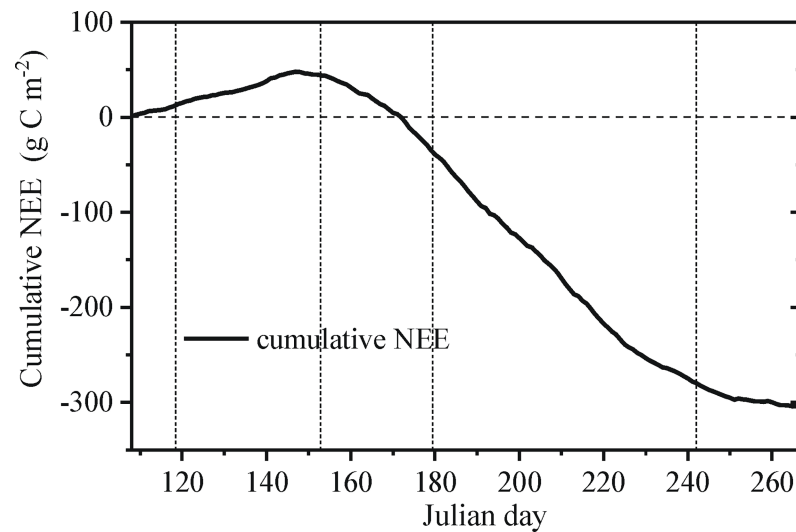
Fig 3. Cumulative time series of total daily NEE (net ecosystem exchange). The vertical dotted lines are the boundaries of different growing stages. The horizontal dotted line represents the zero reference.

cotton field is a carbon source due to little photosynthesis and the predominance of soil respiration. The switch from source to sink is clearly evident around Julian day 148 (Fig 4C); carbon fixation then persists to the end of boll opening, the photosynthesis of cotton being dominant. Over the entire cotton growing season, the cumulative NEE is approximately -304.8 g C m^{-2}.

Variations in daily NEE, R_{eco} and GPP

Overall, the dynamic of NEE, ecosystem respiration (R_{eco}) or GPP shows a single-peak curve in cotton's entire development stage. Over the entire growing season, NEE, R_{eco} and GPP reach a maximum of -6.4 gCm^{-2}d^{-1}, 9.18 gC m^{-2}d^{-1} and 15.19 gC m^{-2}d^{-1}, respectively. The flowering and boll formation period (days 180–242) accounts for 80.58%, 47.68% and 57.60% of the NEE, R_{eco} and GPP, respectively. Each of these percentages is highest during the growing season. Therefore, the fourth period is the primary growth stage. Additionally, the cumulative R_{eco} and GPP are approximately 706.18g C m^{-2}and 1011.00 g C m^{-2}, respectively.

Meteorological characteristics have obvious temporal variability during the growing season (Fig 4A and 4B). Fig 4 shows that the trend of GPP changes corresponding with the change of environmental factors (R_n, T_{air} and VPD, etc.). For instance, irrigation of 4.5 mm on days 201–202 induces the increase of GPP by approximately 3.40%; the low points of R_n and T_{air} in
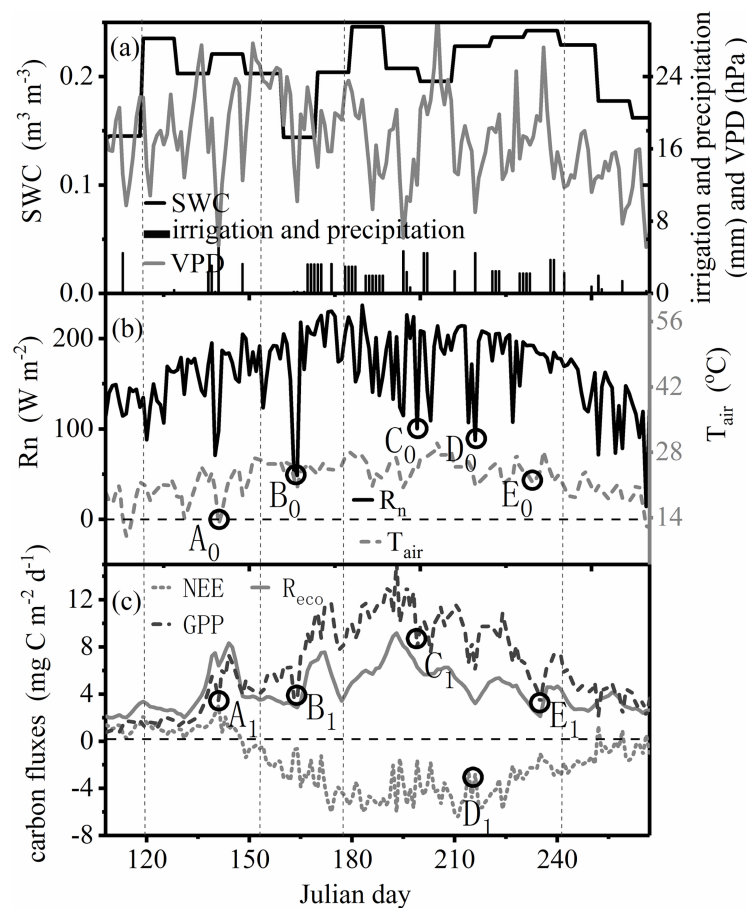
Fig 4. Total daily GPP (gross primary production) and mean daily T_{air} (air temperature), R_n (net solar radiation), rainfall, VPD (vapor pressure deficit) and SWC (soil water content). The vertical dotted lines are the boundaries of different growing stages. The horizontal dotted lines represent the zero reference.

the local region correspond with the local minimum GPP such as A_0 and A_1, B_0 and B_1, and C_0 and C_1. However, there is another situation: as R_n decreases, the GPP increases. Therefore, variability in GPP is related to environmental factors (R_n, T_{air} and SWC) (Fig 4), which are important controlling factors of the carbon balance [53].

Responses of GPP at half-hourly, daily and monthly time scales

At the half-hour time scale, it is assumed that the responses of GPP to each environmental factor is independent of the other variables when values for the other environmental factors are not limiting [54]. The data are selected for the daytime (downward solar radiation > 20 W m^{-2}) of the entire growing season.

As R_n increases, the GPP asymptotically increases from zero to a maximum (Fig 5A) and shows no saturation before R_n increases to 600 W m^{-2}. GPP increases as T_{air} increases to approximately 29°C; GPP then declines slightly, despite T_{air} increasing further (Fig 5B). Likewise, the increase of VPD at the range of 0–22 hPa causes GPP increase and the GPP reaches the maximum when VPD reaches 22 hPa; GPP then declines as VPD increases to more than 22 hPa (Fig 5C). The estimated maximal values for the correlation of GPP to R_n, T_{air} and VPD are 0.72, 0.7 and 0.74 g C m^{-2} half-hourly^{-1}, respectively (Table 1).

Fig 6 shows the responses of the total daily GPP to mean daily environmental variables (R_n, T_{air}, SWC and VPD), using a logistic function ($\ln(y) = ax + b$) for this site.

At the daily time scale, the responses of total daily GPP to mean daily T_{air} and R_n are similar, but total daily GPP shows a stronger correlation with mean daily R_n ($R^2 = 0.396$) than mean daily T_{air} ($R^2 = 0.37$), which are more strongly correlated with total daily GPP than mean daily SWC ($R^2 = 0.08$). Nevertheless, mean daily VPD is weakly correlated with total daily GPP ($R^2 < 0.001$).

At the monthly time scale (Fig 7), using a linear function, total monthly GPP is more strongly correlated with mean monthly T_{air} ($R^2 = 0.88$) than mean monthly R_n ($R^2 = 0.70$), and total monthly GPP is more weakly correlated with mean monthly SWC ($R^2 = 0.21$) than mean monthly T_{air} and R_n. Mean monthly VPD, however, is still poorly correlated with total monthly GPP ($R^2 < 0.001$). Hence, the total monthly GPP is most sensitive to mean monthly T_{air} among these environmental factors.

Fig 8 shows that GPP is more strongly correlated with T_{air} than R_n at time scales of half-hourly to monthly; SWC are weakly correlated with GPP at all time scales. With the scaling up of time from hour to month, the correlations of GPP to T_{air}, R_n and SWC become stronger.
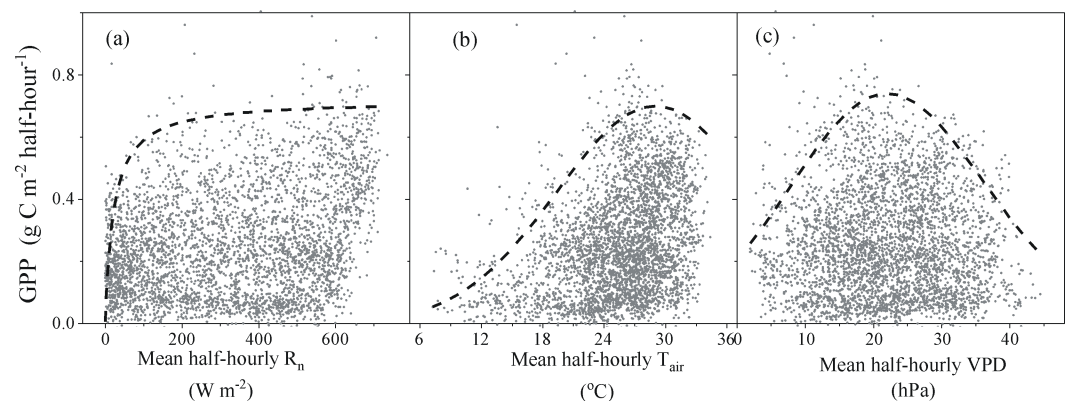
Fig 5. The response curves of total half-hourly GPP (gross primary production) to mean half-hourly R_n (net solar radiation) (a), T_{air} (air temperature) (b), and VPD (vapor pressure deficit) (c) at the 95% confidence interval.

Table 1. Parameters of the responses of the GPP against environmental factors.

	GPP to R_n		GPP to T_{air}				GPP to VPD			
	GPP_{max}	b	GPP_{max}	K_1	K_2	K_3	GPP_{max}	K_1	K_2	K_3
Wulanwusu	0.72	22	0.70	97.43	18000	29	0.74	1.1	419.17	22

GPP_{max} is the saturation point of GPP; b is the rate of GPP; k_1 and k_2 are the dispersion parameters; and k_3 is the optimal value of VPD or T_{air}.

Response of GPP residuals at the daily scale

Some researchers have contended that at the daily scale, GPP could be reliably predicted from R_n and T_{air} [32]. Therefore, the study simulates GPP driven separately by R_n and T_{air} on a daily scale. RH and VPD are strongly correlated with the GPP-R_n relationship (R^2 = 0.40 and 0.17, respectively) (Table 2) and the GPP-T_{air} relationship (R^2 = 0.46 and 0.39, respectively) (Table 3). RH is the most important variable explaining the variability of the residuals and VPD is second (Tables 2 and 3). However, SWC and Ustar have slight impacts on the GPP residuals (Tables 2 and 3). RH, Ustar, and VPD are stronger correlations to the residuals of the GPP-T_{air} relationship than the residuals of the GPP-R_n relationship (Tables 2 and 3).

Discussion

Energy balance closure

Energy balance closure (EBC) is an indicator of quality evaluation for the dataset from EC system [55]. In this study, the energy balance is not closed. The main reasons are neglected energy
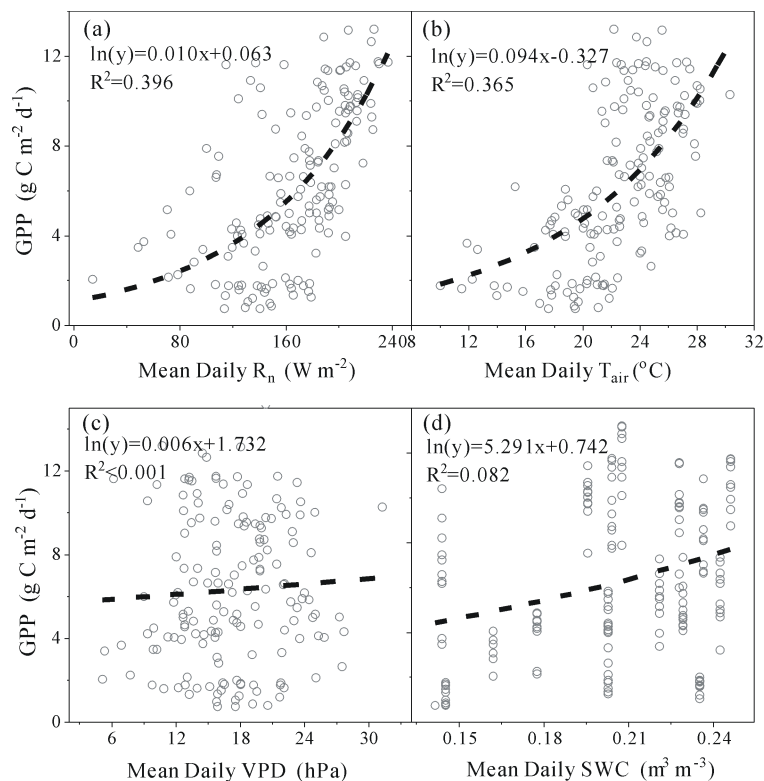
Fig 6. The relationship between total daily GPP (gross primary production) and mean daily R_n (net solar radiation), T_{air} (air temperature), VPD (vapor pressure deficit) and SWC (soil water content), respectively.
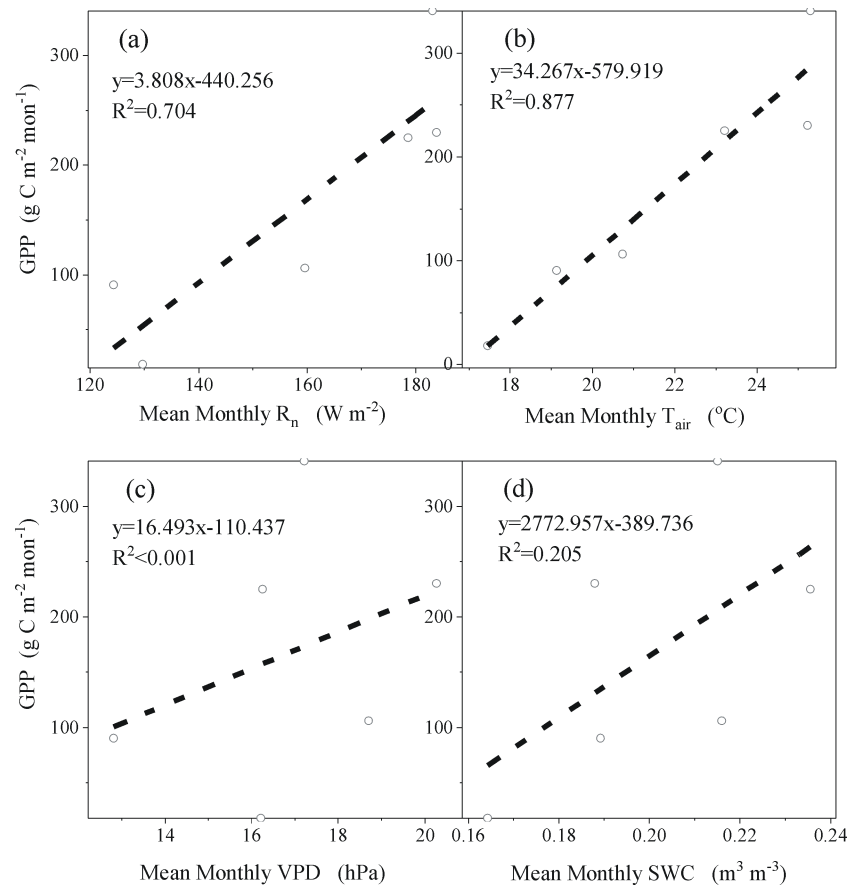
Fig 7. The relationship between total monthly GPP (gross primary production) and mean monthly R_n (net solar radiation), T_{air} (air temperature), VPD (vapor pressure deficit) and SWC (soil water content), respectively.

sinks and horizontal or vertical advection of heat and water vapor, induced by plastic film mulch, which has a great impact on the process of energy partitioning at the soil surface under the plastic film. Plastic film mulch can clearly slow the rates of soil drying; hence, soil under plastic film mulch can maintain more water than bare soil. In the cotton field, bare areas draw water not only vertically from deeper soil layers, but also horizontally from the mulched areas, which act as a "sink" for soil water. The temperature of bare soil is higher than that of mulched soil; therefore, bare areas can act as a heat source for nearby mulched areas [18]. Moreover, condensation on the inside plastic film mulch also occurs because T_{air} above plastic film mulch is higher than under mulch. In consequence, energy transfer in the soil-mulch-atmosphere system is difficult to be acquired by the EC instrument [8, 17, 19], resulting in the non-closure of energy balance. Table 4 shows the energy closure ratios off our typical arid eco-system experimental stations in central Asia. Energy closure ratio in mulched fields is 0.57, clearly less than that in non-mulched fields (CN-FUk, KZ-Ara and KZ-Bal are 0.86, 0.76 and 0.95, respectively) [56]. Therefore, energy balance closure in mulched fields is poorer than that in non-mulched fields. The comparisons further verify that energy balance nonclosure of this study is principally induced by plastic film mulch.

Additionally, variations of leaf area index influence energy partition [57], thereby impacting energy balance closure. A large LAI increases transpiration, which could lessen the vertical water and heat transfer under the film mulch. In the period of flowering and boll forming, LAI
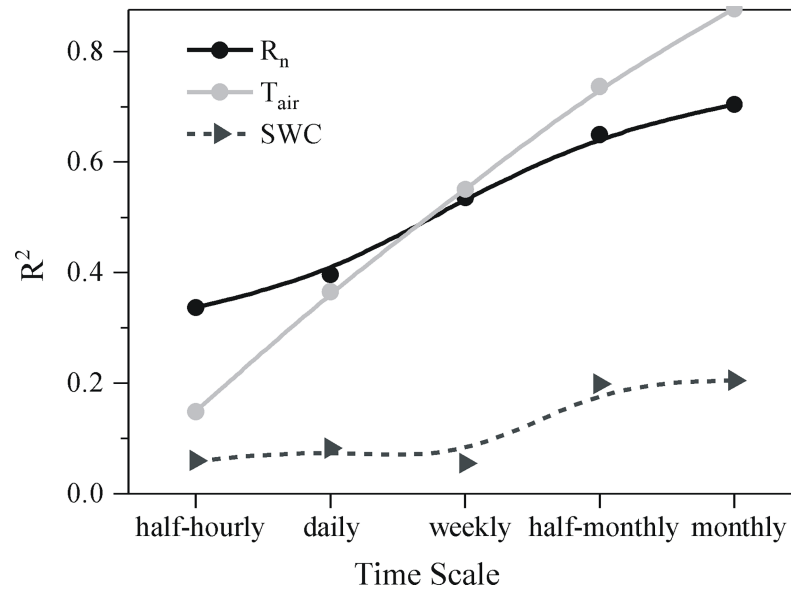
Fig 8. Comparisons of correlations of GPP (gross primary production) to R_n (net solar radiation), T_{air} (air temperature) and SWC (soil water content) at various time scales.

is largest, but energy balance closure is slightly worse than in other stages (Table 5). The reason for this phenomenon is that the interaction of high temperature and stronger solar radiation results in the increasing of VPD and stomata closure to reduce canopy transpiration, thereby increasing the vertical water and heat transfer under the film mulch and then decreasing the energy closure ratio[57].

Variations of GPP, R_{eco} and NEE

The cotton field is regarded as a carbon sink in all growing seasons. Compared with the study of Li et al. [14], the absolute value of the cumulative NEE in the present study is slightly higher than in the non-mulched cotton field without dripped irrigation. Also, Cuello *et al.* [12] also concluded that plastic film mulching increased grain productivity by 8–33% over non-mulching. Plastic mulching can improve soil temperature and SWC, enhance water use efficiency, increase soil microbial activity and the mineralization process, and so on, resulting in increased carbon fixation and nutrients uptake [12, 18, 58–63]. Improving soil temperature and water promotes the growth of crop roots and improves the root distribution across the soil profile [64]. These improvements enhance the ability of crops to extract more nutrients and water from soil [64].

The GPP of terrestrial vegetation is an important variable in determining the global carbon cycle, as well as interannual variation in the atmospheric carbon concentration [65]. Moreover,

Table 2. Relationships between the residuals from the regression of GPP-R_n and environmental variables at the daily time scale.

Variable	Regression equation	R^2
RH	Residuals = 0.140RH-5.91987	0.402
Ustar	Residuals = -67.142Ustar^2+21.762Ustar-1.47297	0.016
VPD	Residuals = -11.004log^2(VPD)+29.911log(VPD)-20.148	0.171
SWC	Residuals = 16.640SWC-3.382	0.032

Table 3. Relationships between the residuals from the regression of GPP-T_{air} and environmental variables at the daily time scale.

Variable	Regression equation	R^2
RH	Residuals = 0.153RH-6.554	0.459
Ustar	Residuals = -78.215Ustar^2+23.694Ustar-1.496	0.030
VPD	Residuals = -19.991log^2(VPD)+37.148log33-15.403	0.214
SWC	Residuals = 19.471SWC-4.037	0.043

the responses of GPP to environmental factors are similar to the responses of NEE or R_{eco} [66]. More importantly, GPP is the acquisition of net carbon by photosynthesis, the process by which carbon and energy enter an ecosystem, and the best measure of the carbon that enters the ecosystem [66]. Therefore, the study uses GPP to analyze the responses of carbon fluxes to environmental factors (R_n, T_{air}, VPD, SWC and Ustar).

Responses of GPP at half-hourly, daily and monthly time scales

At the half-hourly time scale, on the condition that other environmental factors are optimal, the boundary curves show the response of the dependent variable (GPP) to an independent variable (R_n, T_{air} or VPD) and can describe the relations of GPP to a single meteorological factor. For instance, at low levels of R_n, the energy supply limits GPP, but at high levels of R_n, other factors (especially SWC and the hydraulic conductance of soil and plant) limit the GPP. When R_n reaches 600W m^{-2}, photosynthesis reaches saturation due to the limited ability of light-harvesting; at extremely high levels of R_n, photosynthesis decreases due to photo oxidation of photosynthetic enzymes and pigments.

In arid regions, soil moisture, to a large extent, relies on T_{air} [34]. Because plastic mulching retains the soil moisture and the cotton is regularly irrigated, soil moisture is not the limiting factor for the entire growth season [8]. Furthermore, the increase of VPD induces an increase of the evaporative demand [54] and stomatal limitation to an increase in carbon fixation in the range of 0–22 hPa. However, the decrease of stomata conductance does not induce a decrease of C fixation in the range of 0–22 hPa due to the increasing of water use efficiency of photosynthesis. When VPD > 22hPa, the increase of VPD induces an increase of evaporative demand. When the evaporative demand can not be met, the stomata close and flux rates decline to match the water constraint [53]. Nevertheless, the optimal VPD (22hPa) in a drip-irrigated, film-mulched cotton field is higher than in wet–dry–tropical savanna (10-20hPa) without film mulching and drip-irrigation [67].

Under high soil water potential, carbon fixation does not respond to an increase in VPD [68]; under moderate and severe water stress, carbon fixation is significantly reduced with

Table 4. Energy closure ratio comparsions of mulched cotton in the Wulanwusu and non-mulched vegetations in other areas.

Experimental station	Main vegetation type	Year(month)	Energyclosure ratio[4]	Mulch or non-mulched	Source
Wulanwusu	Cotton	2012(4–10)	0.57	yes	This study
CN-Fuk[1]	*Tamarix ramosissima*	2009(4–10)	0.86	no	Wang
KZ-Ara[2]	*Halostachys caspica and Tamarix chinensis*	2012(5–8)	0.76	no	Wang
KZ-Bal[3]	grassland	2012(5–9)	0.95	no	Wang

[1]CN-Fuk (Fukang Desert Ecosystem Observation and Experiment Station, Chinese Academy of Sciences) is located in Xinjiang, China.

[2] KZ-Ara is located in Aral Lake, Kazakhstan

[3]KZ-Bal is located in Balkhash Lake, Kazakhstan

[4]Energy closure ratio (slope of LE+H against R_n-G) represents the degree of energy balance closure.

Table 5. LAI comparison for each of the growth stages.

	N	R^2	Slope	LAI	Julian day
Sowing seed	527	0.919	0.569		108–118
Seed emergence	1680	0.906	0.578	0.3	119–153
Squaring	1248	0.920	0.607	0.5	154–179
Flowering and boll formation	3024	0.906	0.553	2.3	180–242
				3.7	
				4.5	
Boll opening	1200	0.946	0.606	4	243–267
				2.3	

N represents the number of records of carbon flux.

increasing VPD [69]. Film mulch decreases water stress, so the optimal VPD corresponding with the maximum GPP is high in this study. Bai *et al.* [51] used 4-year data (2009, 2010, 2012 and 2013) at the same station and found that film mulched drip irrigation effected the relationship between GPP and environmental factors, such as R_n, T_{air} and VPD.

The correlations of GPP to T_{air}, R_n and SWC become stronger with time scaling up from half-hour to month (Fig 8). From the perspective of ecology, an ecosystem has the characteristics of resistance and resilience. Resilience is a measure of robustness and buffering capacity of the ecosystem to changing conditions [70]. Plant photosynthesis and growth maintain high resilience in the face of diurnal and seasonal variations [66]. Additionally, plastic film mulch can enhance ecosystem resistance because plastic film mulch can reduce soil erosion and control weeds [12]. Ona short time scale, the fluctuation of GPP is large in the face of changes toR_n, T_{air} and SWC because GPP immediately responds to these perturbations; ona long time scale, GPP tends to be stable due to ecosystem resistance and resilience. Therefore, the data of GPP at a short time scale are more discrete than at a long time scale, resulting in a stronger correlation at a longtime scale. From a statistical point of view, a longtime scale can filter out some outliers of GPP and climate data and make data deviations diminish. However, the correlation of VPD to GPP is especially weak at all time scales in this region. The reason is that the protection of plastic film mulch and regular irrigation allow soil maintain sufficient water [8], and with sufficient soil water, VPD has little effect on photosynthesis [71].

Ona short time scale, the correlation of GPP to R_n is more sensitive than to T_{air}; ona long time scale, it reverses (Fig 8). This phenomenon is determined by the biochemical characteristics of photosynthesis [66]. The most conspicuous characteristics of carbon-fixation reaction are that: photosynthetic enzymes need a great amount of nitrogen; carbon fixation depends on the products of the light-harvesting reaction (ATP and NADPH) which, in turn, depends on solar radiation; and carbon fixation is restricted by the supply of carbon dioxide [66]. The chloroplasts of leaves respond to the change of available light in a few minutes [66]. However, it takes a few days or weeks for the changes of the density of light-harvesting pigment and photosynthetic enzymesto take effect. Moreover, temperature has a great effect on the content of plant nitrogen [72]; high temperature enhances the potential of soil nitrfication and increases the openness of the soil nitrogen cycle [73]. Plastic film mulching can also improve nitrogen availability for a plant increasing the density of photosynthetic enzymes gradually. Therefore, radiation and the supply of carbon dioxide are extremely sensitive to this process at time scales of milliseconds to minutes; T_{air} is sensitive to this process at time scale of days to weeks.

However, SWC is more weaklycorrelated with GPP than R_n and T_{air} at all time scales. Plastic film mulching blocks parts of energy transfer from soil to air and diminishes the impact of

changes of SWC on T$_{air}$ by soil thermal characteristics, resulting in weekly correlation of SWC to the GPP residuals. At the same time, deep roots of cotton in arid region extract water from the capillary fringe of the water table, and stored water in the stem can ease the supply and demand imbalance of water [66]. Plastic film mulch can also improve soil water if the cotton is regularly irrigated. Therefore, providing enough soil water with cotton scarcely induces the decreasing of stomatal conductance so that GPP is unresponsive to SWC [67].

Ustar is also poorly related with GPP, as shown in Tables 2 and 3. Plastic film mulching reduces Ustar, and hence the rate of wind on the surface increases. Wind can accelerate the diffusion of carbon dioxide from the atmosphere to leaves, resulting in the increasing of carbon fixation, but strong light in arid region increases stomatal conductance; then, the limitation of the density of carbon dioxide to photosynthesis is reduced to a minimum, and Ustar and wind decrease the GPP residuals.

From the perspective of resource allocation, enviromental changes, such as the fluctuation of nutrient supply and storms, vary the relative abundance of resources. Therefore, it is inevitable that there are different limiting factors for carbon fluxes at different time scales [66].

Conclusions

Drip irrigation under plastic mulch is widely used in Xinjiang, the largest arid region in China. This study investigated the relationships between carbon fluxes and environmental factors in a drip-irrigated, film-mulched cotton field of this water-limited region. The cotton field is a strong sink of carbon, and its cumulative NEE over the entire growing season is -304.8 g C m^{-2}. The cumulative NEE in mulched cotton field is higher than that in non-mulched cotton field. RH, R$_n$, and T$_{air}$ are important controlling factors of carbon balance, RH was the most limiting environmental factor. However, SWC and Ustar have slight impacts on the GPP residuals. Additionally, RH, Ustar and VPD are slightly more correlated with the simulated GPP driven by T$_{air}$ than by R$_n$. RH, VPD and Ustar are more sensitive to T$_{air}$ than R$_n$ [66]. High temperature decreases RH and increases VPD. Decreasing of Ustar increases the rate of wind and evaporation, which decreases leaf temperature [66]. In general, the total daily GPP could be reliably predicted from R$_n$ and T$_{air}$; at the same time, RH, Ustar, SWC and VPD are also important factors to constrain the response of GPP to R$_n$ and T$_{air}$ at different degrees of limitation.

Supporting information

S1 File. The minimal data set. This file includes the data of Fig 1–7.
(XLSX)

Author Contributions

Conceptualization: Yan Li.

Data curation: Xiaoyu Li, Lijuan Liu.

Formal analysis: Xiaoyu Li, Huijin Yang.

Funding acquisition: Xiaoyu Li.

Methodology: Lijuan Liu, Huijin Yang.

Project administration: Xiaoyu Li.

Resources: Lijuan Liu.

Supervision: Yan Li.

Writing – original draft: Xiaoyu Li, Huijin Yang.

Writing – review & editing: Xiaoyu Li, Lijuan Liu, Huijin Yang, Yan Li.

References

1. Watson RT, Zinyowera MC, Moss RH. Climate Change 1995 impacts, adaptations and mitigation of climate change: Scientific-technical analysis. Cambridge: Cambridge University Press; 1996.

2. Smith P, Martino D, Cai Z, Gwary D, Janzen H, Kumar P, et al. Greenhouse gas mitigation in agriculture. Philos Trans R Soc, Ser. B: Biological Sci. 2008; 363:789–813.

3. Watson R., Rodhe H, Oeschger H, Siegenthaler U. Greenhouse gases and aerosols. Climate change: the IPCC scientific assessment. Cambridge: Cambridge University Press; 1990.

4. Yoshimoto M, Oue H, Kobayashi K. Energy balance and water use efficiency of rice canopies under free-air CO_2 enrichment. Agr Forest Meteorol. 2005; 133:226–46.

5. Baker JT, Van Pelt S, Gitz DC, Payton P, Lascano RJ, McMichael B. Canopy gas exchange measurements of cotton in an open system. Agron J. 2009; 101:52–9.

6. Tubiello FN, Rosenzweig C, Kimball BA, Pinter PJ, Wall GW, Hunsaker DJ, et al. Testing CERES-wheat with free-air carbon dioxide enrichment (FACE) experiment data: CO_2 and water interactions. Agron J. 1999; 91:247–55.

7. Oelbermann M, Paul Voroney R, Gordon AM. Carbon sequestration in tropical and temperate agroforestry systems: a review with examples from Costa Rica and southern Canada. Agric Ecosyst Environ. 2004; 104:359–77.

8. Zhou S, Wang J, Liu J, Yang J, Xu Y, Li J. Evapotranspiration of a drip-irrigated, film-mulched cotton field in northern Xinjiang, China. Hydrol Process. 2012; 26:1169–78.

9. Zhang Q, Xu H, Li Y. Oasis evolution and water resource utilization of a typical area in the inland river basin of an arid area: a case study of the Manas River valley. Environ Earth Sci. 2012; 66:683–92.

10. Ling H, Xu H, Fu J, Fan Z, Xu X. Suitable oasis scale in a typical continental river basin in an arid region of China: A case study of the Manas River Basin. Quatern Int. 2013; 286:116–25.

11. Wu J, Guo W, Feng J, Li L, Yang H, Wang X, et al. Greenhouse Gas Emissions from Cotton Field under Different Irrigation Methods and Fertilization Regimes in Arid Northwestern China. The Scientific World J. 2014; 2014:1–10.

12. Cuello JP, Hwang HY, Gutierrez J, Kim SY, Kim PJ. Impact of plastic film mulching on increasing greenhouse gas emissions in temperate upland soil during maize cultivation. Appl Soil Ecol. 2015; 91:48–57.

13. Li Z. Effects of plastic film mulching with drip irrigation on N_2O and CH_4 emissions from cotton fields in arid land. J Agric Sci. 2014; 152:534–42.

14. Li Z, Zhang R, Wang X, Wang J, Zhang C, Tian C. Carbon dioxide fluxes and concentrations in a cotton field in Northwestern China: effects of plastic mulching and drip irrigation. Pedosphere. 2011; 21:178–85.

15. Yang Q, Zuo H, Xiao X. Modelling the effects of plastic mulch on water, heat and CO_2 fluxes over cropland in an arid region. J Hydrol. 2012; 452:102–18.

16. Zhang F, Li M, Qi J, Li F, Sun G. Plastic Film Mulching Increases Soil Respiration in Ridge-furrow Maize Management. Arid Land Res Manag. 2015; 29:432–53.

17. Wu Y, Perry KB, Ristaino JB. Estimating temperature of mulched and bare soil from meteorological data. Agr Forest Meteorol. 1996; 81:299–323.

18. Bristow KL, Horton R. Modeling the impact of partial surface mulch on soil heat and water flow. ThApC. 1996; 54:85–98.

19. De Luca V, Ruocco G. SW—Soil and Water: A Transient-spectral Thermal Model of Soil under Radiative-interfering Cover. JAER. 2000; 77:93–102.

20. Liu C, Li F, Zhou L, Feng Q, Li X. Effects of water management with plastic film in a semi-arid agricultural system on available soil carbon fractions. Eur J Soil Biol. 2013; 57:9–12.

21. Liu Y, Li S, Yang S, Hu W, Chen X. Diurnal and seasonal soil CO_2 flux patterns in spring maize fields on the Loess Plateau, China. Acta Agric Scand Sect B, Soil and Plant Sci. 2010; 60:245–55.

22. Wang G, Liang Y, Zhang Q, Jha S, Gao Y. Mitigated CH_4 and N_2O emissions and improved irrigation water use efficiency in winter wheat field with surface drip irrigation in the North China Plain. Agric Water Manage. 2016; 163:403–7.

23. Berger S, Kim Y, Kettering J, Gebauer G. Plastic mulching in agriculture—Friend or foe of N_2O emissions? Agric Ecosyst Environ. 2013; 167:43–51.

24. Baldocchi D, Falge E, Gu L, Olson R, Hollinger D, Running S, et al. FLUXNET: A new tool to study the temporal and spatial variability of ecosystem-scale carbon dioxide, water vapor, and energy flux densities. B Am Meteorol Soc. 2001; 82:2415–34.

25. Bergeron O, Margolis HA, Black TA, Coursolle C, Dunn AL, Barr AG, et al. Comparison of carbon dioxide fluxes over three boreal black spruce forests in Canada. Global Change Biol. 2007; 13:89–107.

26. Beringer J, Livesley SJ, Randle J, Hutley LB. Carbon dioxide fluxes dominate the greenhouse gas exchanges of a seasonal wetland in the wet–dry tropics of northern Australia. Agr Forest Meteorol. 2013; 182:239–47.

27. Broeckx LS, Verlinden MS, Berhongaray G, Zona D, Fichot R, Ceulemans R. The effect of a dry spring on seasonal carbon allocation and vegetation dynamics in a poplar bioenergy plantation. GCB Bioenergy. 2014; 6:472–87.

28. Kolari P, Pumpanen J, Rannik Ü, Ilvesniemi H, Hari P, Berninger F. Carbon balance of different aged Scots pine forests in Southern Finland. Global Change Biol. 2004; 10:1106–19.

29. Niu S, Luo Y, Fei S, Montagnani L, Bohrer G, Janssens IA, et al. Seasonal hysteresis of net ecosystem exchange in response to temperature change: patterns and causes. Global Change Biol. 2011; 17:3102–14.

30. Saigusa N, Yamamoto S, Hirata R, Ohtani Y, Ide R, Asanuma J, et al. Temporal and spatial variations in the seasonal patterns of CO_2 flux in boreal, temperate, and tropical forests in East Asia. Agr Forest Meteorol. 2008; 148:700–13.

31. Tong X, Zhang J, Meng P, Li J, Zheng N. Ecosystem water use efficiency in a warm-temperate mixed plantation in the North China. J Hydrol. 2014; 512:221–8.

32. Vourlitis GL, Oechel WC, Hope A, Stow D, Boynton B, Verfaillie J, et al. Physiological models for scaling plot measurements of CO_2 flux across an arctic tundra landscape. Ecol Appl. 2000; 10: 60–72.

33. Whitley R, Medlyn B, Zeppel M, Macinnis-Ng C, Eamus D. Comparing the Penman–Monteith equation and a modified Jarvis–Stewart model with an artificial neural network to estimate stand-scale transpiration and canopy conductance. J Hydrol. 2009; 373:256–66.

34. Baldocchi D. 'Breathing' of the terrestrial biosphere: lessons learned from a global network of carbon dioxide flux measurement systems. Aust J Bot. 2008; 56:1–26.

35. Aubinet M, Grelle A, Ibrom A, Rannik Ü, Moncrieff J, Foken T, et al. Estimates of the annual net carbon and water exchange of forests: the EUROFLUX methodology. AdvEcol Res. 2000; 30:113–175.

36. Velasco E, Pressley S, Allwine E, Westberg H, Lamb B. Measurements of CO_2 fluxes from the Mexico Cityurban landscape. Atmos Environ. 2005; 39:7433–46.

37. Webb EK, Pearman GI, Leuning R. Correction of flux measurements for density effects due to heat and water vapour transfer. QJRMS. 1980; 106:85–100.

38. Burba G, Anderson D, Xu L, McDermitt D. Correcting apparent off-season CO_2 uptake due to surface heating of an open path gas analyzer: progress report of an ongoing study. 27th Confercence on Agricultural and Forest Meteorology. Boston: American Meteorological Society; 2006.

39. Antonia RA, Mi J. Corrections for velocity and temperature derivatives in turbulent flows. ExFl. 1993; 14:203–8.

40. Béziat P, Ceschia E, Dedieu G. Carbon balance of a three crop succession over two cropland sites in South West France. Agr Forest Meteorol. 2009; 149:1628–45.

41. Flanagan LB, Wever LA, Carlson PJ. Seasonal and interannual variation in carbon dioxide exchange and carbon balance in a northern temperate grassland. Global Change Biol. 2002; 8:599–615.

42. Li Z, Yu G, Wen X, Zhang L, Ren C. Energy balance closure at China FLUX sites. Sci China Ser D. 2005; 34:46–56.

43. Zhu Z, Sun X, Wen X, Zhou Y, Tian J, Yuan G. Study on the processing method of nighttime CO2 eddy covariance flux data in ChinaFLUX. Sci China Ser D. 2006; 49:36–46.

44. Lei HM, Yang DW. Seasonal and interannual variations in carbon dioxide exchange over a cropland in the North China Plain. Global Change Biol. 2010; 16:2944–57.

45. Goulden ML, Munger JW, Fan SM, Daube BC, Wofsy SC. Measurements of carbon sequestration by long-term eddy covariance: Methods and a critical evaluation of accuracy. Global Change Biol. 1996; 2:169–82.

46. Baldocchi D. Assessing the eddy covariance technique for evaluating carbon dioxide exchange rates of ecosystems: past, present and future. Global Change Biol. 2003; 9:479–92.

47. Reichstein M. On the separation of net ecosystem exchange into assimilation and ecosystem respiration: review and improved algorithm. Global Change Biol. 2005; 11:1424–39.

48. Jaksic V, Kiely G, Albertson J, Oren R, Katul G, Leahy P, et al. Net ecosystem exchange of grassland in contrasting wet and dry years. Agr Forest Meteorol. 2006; 139:323–34.

49. Ge ZM, Kellomäki S, Zhou X, Wang KY, Peltola H. Evaluation of carbon exchange in a boreal coniferous stand over a 10-year period: An integrated analysis based on ecosystem model simulations and eddy covariance measurements. Agr Forest Meteorol. 2011; 151:191–203.

50. Whitley R, Taylor D, Macinnis-Ng C, Zeppel M, Yunusa I, O'Grady A, et al. Developing an empirical model of canopy water flux describing the common response of transpiration to solar radiation and VPD across five contrasting woodlands and forests. Hydrol Process. 2013; 27:1133–46.

51. Bai J, Wang J, Chen X, Luo G, Shi H, Li L, et al. Seasonal and inter-annual variations in carbon fluxes and evapotranspiration over cotton field under drip irrigation with plastic mulch in an arid region of Northwest China. J Arid Land. 2015; 7:272–84.

52. Wilson K, Goldstein A, Falge E, Aubinet M, Baldocchi D, Berbigier P, et al. Energy balance closure at FLUXNET sites. Agr Forest Meteorol. 2002; 113:223–43.

53. Williams M, Malhi Y, Nobre A, Rastetter E, Grace J, Pereira M. Seasonal variation in net carbon exchange and evapotranspiration in a Brazilian rain forest: a modelling analysis. Plant, Cell Environ. 1998; 21:953–968.

54. Whitley R, Zeppel M, Armstrong N, Macinnis-Ng C, Yunusa I, Eamus D.A modified Jarvis-Stewart model for predicting stand-scale transpiration of an Australian native forest. Plant Soil. 2008; 305:35–47.

55. Giasson MA, Coursolle C, Margolis HA. Ecosystem-level CO_2 fluxes from a boreal cutover in eastern Canada before and after scarification. Agr Forest Meteorol. 2006; 140:23–40.

56. Wang Y, Jing C, Bai J, Li L, Chen X, Luo G. Characteristics of water and carbon fluxes during growing season in three typical arid ecosystems in central Asia. Chin J Plant Ecol. 2104; 38:795–808. Chinese.

57. Baldocchi D, Meyers T. On using eco-physiological, micrometeorological and biogeochemical theory to evaluate carbon dioxide, water vapor and trace gas fluxes over vegetation: a perspective. Agr Forest Meteorol. 1998; 90:1–25.

58. An T, Schaeffer S, Li S, Fu S, Pei J, Li H, et al. Carbon fluxes from plants to soil and dynamics of microbial immobilization under plastic film mulching and fertilizer application using^{13}C pulse-labeling. Soil Biol Biochem. 2015; 80:53–61.

59. Li S, Wang Z, Li S, Gao Y, Tian X. Effect of plastic sheet mulch, wheat straw mulch, and maize growth on water loss by evaporation in dryland areas of China. Agric. Water Manage. 2013; 116:39–49.

60. Liao Y, Zhang D, Jia Z, Zhang L, Lu Y. Effects of plastic film mulching of millet on soil moisture and temperature in semi-arid areas in south Ningxia of China. Agric Sci Chin. 2004; 4:865–71.

61. Zhang S, Li P, Yang X, Wang Z, Chen X. Effects of tillage and plastic mulch on soil water, growth and yield of spring-sown maize. Soil Till Res. 2011; 112:92–7.

62. Zhou L, Zhang F, Liu C. Improved yield by harvesting water with ridges and subgrooves using buried and surface plastic mulchs in a semiarid area of China. Soil Till Res. 2015; 150:21–9.

63. Li YS. Influence of continuous plastic film mulching on yield, water use efficiency and soil properties of rice fields under non-flooding condition. Soil Till Res. 2007; 93:370–8.

64. Zhou L, Zhang F, Liu C. Ridge-furrow and plastic-mulching tillage enhances maize–soil interactions: Opportunities and challenges in a semiarid agroecosystem. Field Crops Res. 2012; 126:181–8.

65. Cai W, Yuan W, Liang S, Zhang X, Dong W, Xia J, et al. Improved estimations of gross primary production using satellite-derived photosynthetically active radiation. JGR. 2014; 119:110–23.

66. Chapin III FS, Matson PA, Mooney HA. Principles of terrestrial ecosystem ecology. New York: Springer-Verlag; 2002.

67. Whitley R, Macinnis-Ng C, Hutley L, Beringer J, Zeppel M. Is productivity of mesic savannas light limited or water limited? Results of a simulation study. Global Change Biol. 2011; 17:3130–49.

68. Xue Q, Weiss A, Arkebauer TJ, Baenziger PS. Influence of soil water status and atmospheric vapor pressure deficit on leaf gas exchange in field-grown winter wheat. Environ Exp Bot. 2004; 51:167–79.

69. Conaty WC, Mahan JR, Neilsen JE, Constable GA. Vapour pressure deficit aids the interpretation of cotton canopy temperature response to water deficit. Funct Plant Biol. 2014; 41:535–46.

70. Hollings S. Resilence of Ecosystems: Local Surprise and Global Change. Cambridge: Cambridge University Press; 1985.

71. Li J. Response of stomatal conductance and phytohormones of leaves to vapor pressure deficit in some species of plants [dissertation].Jinan: Shandong University; 2014. Chinese.

72. Miller AE, Bowman WD. Variation in nitrogen-15 natural abundance and nitrogen uptake traits among co-occurring alpine species: do species partition by nitrogen form? Oecologia. 2002; 130:609–16. https://doi.org/10.1007/s00442-001-0838-8 PMID: 28547264

73. Liu X. Progress of research on relationships between terrestrial plant nitrogen isotope composition and climate environment change. Adv Earth Sci. 2014; 29:216–226. Chinese.